Jets into liquid under gravity

By D. D. JOSEPH, K. NGUYEN

Department of Aerospace Engineering and Mechanics, The University of Minnesota,
Minneapolis, MN 55455

AND J. E. MATTA

Aberdeen Proving Ground, Maryland 21018

We study the flow of a heavy, viscous, possibly non-Newtonian axisymmetric jet of liquid of density ρ falling under gravity g into a lighter liquid of density $\tilde{\rho}$. If the change in the momentum of the entrained lighter liquid is neglected the jet will ultimately reach a modified Torricelli limit with a speed given by

$$U(x) = \left[2\frac{\delta\rho}{\rho}gx \right]^{\frac{1}{2}}$$

and an asymptotic radius

$$a(x) = \left[\frac{2Q^2}{(\delta\rho/\rho)gx} \right]^{\frac{1}{4}}, \tag{1}$$

where x is the downstream distance, $\delta\rho = \rho - \tilde{\rho} > 0$ and $2Q$ is the volume flow. An exact asymptotic solution perturbing the Torricelli limit with effects of surface tension, viscosity and elasticity is given in powers of $x^{-\frac{1}{4}}$. An extended unsteady problem including effects of entrainment is formulated in terms of nonlinear ordinary differential equations which also account for weak radial variations of the velocity across the cross-section of the jet. These equations are solved in a boundary-layer approximation which gives

$$a(x) \approx 1\cdot171 \left(\frac{\tilde{\rho}}{x}\right)^{\frac{1}{20}} \frac{Q^{\frac{3}{10}}\tilde{\mu}^{\frac{1}{5}}}{(\delta\rho\, g)^{\frac{1}{4}}}, \tag{2}$$

where $\tilde{\mu}$ is the viscosity of the ambient fluid. Equation (1) is in agreement with experimental observations of jets of liquid into air. Equation (2) is in agreement with experimental observations of jets of liquids into liquids.

1. Introduction

A heavy, possibly non-Newtonian, liquid of density ρ is extruded from a pipe or vessel of radius a_0 into a lighter fluid of density $\tilde{\rho}$. It is assumed that flow in the jet is axisymmetric with velocity

$$\mathbf{U}(x, r) = \mathbf{e}_x\, U(x, r) + \mathbf{e}_r\, W(x, r)$$

and radius $r = a(x)$, where x increases downward in the direction of gravity (see figure 1). It is further assumed that the viscosity of the jet is very much larger than the viscosity of the ambient fluid. This implies that the variation of U is determined by the internal dynamics of the jet, and ultimately, for large x, the accelerating jet will thin out and $U(x, r)$ will become independent of r. The falling jet will entrain ambient fluid, however, even if the viscosity $\tilde{\mu}$ of the ambient liquid is small, and the change

of momentum of entrained fluid will be very important if the density of the entrained liquid is not too small. Thus there are two cases:

(i) the entrainment effect is not important – this case is realized perfectly for jets into vacuum, and it is realized in practice in the case of jets of liquid into air;

(ii) the entrainment effect is important – this case is realized when liquids are extruded into liquids.

The two cases are qualitatively different in that the leading dynamical balances, in asymptotic regions, are between the relative weight of the jet per unit length and its change of momentum in case (i), and between the relative weight of the jet and the change of momentum of the entrained liquid in case (ii). Equations (1.1) and (1.2) below show that there is a huge difference between these two cases. Our experiments show that both cases are realizable.

We treat case (i) under the mathematical assumption that the ambient fluid is inviscid and dynamically passive. This means that the stress exerted on the heavy liquid by the light one is hydrostatic. The effect of the hydrostatic pressure is to reduce gravity g to $(\delta\rho/\rho)g$, where $\delta\rho$ is the difference in density. Thus, any result for flow of a liquid in air or a vacuum which depends on the gravity g also describes the flow in another (dynamically inactive) liquid when g is replaced with $\delta\rho g/\rho$. In the case of vertical jets into liquid we get the effect of gravity as a constant acceleration of the jet which reaches finally a terminal speed given by the asserted modification $[2(\delta\rho/\rho)gx]^{\frac{1}{2}}$ of Torricelli's formula $(2gx)^{\frac{1}{2}}$. The radius of the jet must then get smaller and smaller, reaching ultimately the asymptotic radius

$$a(x) \sim \left[\frac{2Q^2}{(\delta\rho/\rho)gx}\right]^{\frac{1}{4}}. \tag{1.1}$$

We find a formally exact asymptotic solution of viscous, non-Newtonian equations in powers of $x^{-\frac{1}{4}}$. We work with a nonlinear jet-shape equation derived from the equation of motion. The same results follow from direct exact analysis of the governing partial differential equation. The algorithm for computing such an exact solution in the case of Newtonian jets into air was indicated by Kaye & Vale (1969), but they obtained only the first two terms of the asymptotic series. Kaye & Vale found that their asymptotic solution was good for an oil of low but not of high viscosity. For the high-viscosity oil they studied a nonlinear jet-shape equation (see (6.23)) which is a special case of (5.18) and got good agreements. They called the asymptotic method (II) and the method of integration of the jet-shape equation (I), and maintained that there was a strong distinction between the two methods. In fact, their method (I) is the same as (II) when the surface-tension terms are added to (I) and x is large. Clarke (1969) treats viscous fluids with surface tension and he has derived the correct three-term asymptotic expansion (5.19). He uses a hodograph method with streamline coordinates, so his analysis, which is based on some unnecessary assumption about small parameters, and the expression of his results are less direct and appear to be less rigorous than our analysis shows they actually are.

The fluid dynamics of the jet near the exit (say, within 2 or 3 diameters) is more complicated because the flow must adjust from a distribution compatible with flow in a pipe to flow in a jet. This problem is usually studied with $g = 0$ (see e.g. Trogdon & Joseph 1980, 1981). In this case the flow reaches a uniform velocity and a final swelled radius (larger than the pipe radius – much larger for some viscoelastic jets (see figures 2 e–g). So the limit $\delta\rho \to 0$ might be expected to coincide with the problem of die swell as it is usually formulated. There is nothing to accelerate the jet when the densities are matched and, in principle, the jet diameter will not vary downstream (actually the jet will eventually be destroyed by instabilities not considered here).

It is not uncommon to simulate $g = 0$ in experiments on die swell by density matching, but the idea behind that experimental technique can be erroneous if it neglects the effects of entrainment of the ambient fluid by viscous action. In fact the rate of change of the momentum of the entrained fluid, which in any case is small if the density of the entrained fluid is small, can be large when density of the lighter liquid is comparable to the density of the liquid in the jet. In this case (2) the overall change of momentum produces smaller velocities and larger jets so that the swelled radius computed in case (1) for small values of $\delta \rho\, g$ may be much smaller than those that are actually observed. It could be said that there is a 'die swell' which is associated with entrainment of the ambient liquid.

The dynamical effects of entrainment of ambient liquid by the jet are studied in §§6 and 7. We derive some nonlinear ordinary differential equations for jet problems which are axisymmetric but unsteady. These equations differ from approximate equations used in the problem of fibre spinning, and other thin-fluid filament problems in that the dynamics of the ambient liquid is represented and the equations allow at least for weak radial variations of the velocity and pressure at each axial station. In §7 we treat the problem of entrainment by approximate methods in which the dynamics of the entrained liquid is presumed to be governed by boundary-layer equations, and the boundary-layer equations are studied by the method of Kármán and Pohlhausen. We find that the boundary-layer thickness increases like $1/a^3$ and that ultimately the jet radius is nearly constant and is given by

$$a(x) = 1 \cdot 171 \left(\frac{\tilde{\rho}}{x}\right)^{\frac{1}{20}} \frac{Q^{\frac{3}{10}} \tilde{\mu}^{\frac{1}{5}}}{(\delta\rho\, g)^{\frac{1}{4}}}. \tag{1.2}$$

The results from theoretical analysis seem to be in good agreement with observations reported in §2 and discussed in §§5 and 8.

2. Experiments

In our experiments we extruded heavy liquids from a round pipe of radius $r = a_0$, with vertical x-axis parallel to gravity, into lighter fluids of different densities $\tilde{\rho}$. The experiments were originally undertaken to study the problem of 'die swell' in non-Newtonian fluids. This led us to certain problems in understanding the influence of the ambient liquid on the dynamics of the jet. A partial resolution of these problems is established in the theory developed in the sequel. To motivate our theory it is perhaps best to report some details of the actual motions that we observed in our experiments.

A sketch of a typical experiment is shown below in figure 1. In this work the density difference $\rho - \tilde{\rho} > 0$ is of crucial importance. We have normalized this density difference with the density ρ of the extruded liquid

$$\epsilon \equiv \frac{\rho - \tilde{\rho}}{\rho}. \tag{2.1}$$

In a vacuum $\tilde{\rho} = 0$ and $\epsilon = 1$, $\epsilon \approx 1$ when $\tilde{\rho}$ is for air and ϵ is very small when the density $\tilde{\rho}$ of the lighter ambient liquid is close to ρ. Unfortunately it is not possible to find ambient fluids of intermediate density. We can extrude into a gas or a liquid. There is nothing in between. Fortunately, we can at least find liquids of different density so that different but small values ϵ can be used to test our theory.

We worked with jets of silicone oil and jets of an elvacite solution into air and into liquids of different density. The silicone oil is a Newtonian liquid which swells a little at the exit and the elvacite solution is a viscoelastic liquid which swells a lot at the
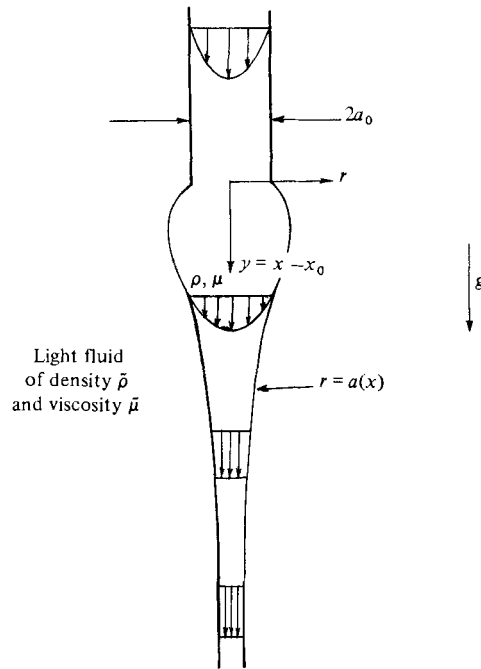
FIGURE 1. Sketch of the falling jet. For large x the jet radius and
the radial velocity tend to zero.

Ambient fluid	Density difference silicone 1 (g/cm^3)	Viscosity of ambient fluid (cP)
Air	0·943	—
100 % alcohol	0·161	1·2
71 % alcohol/water	0·068	2·3
50 % alcohol/water	0·023	2·8
40 % alcohol/water	0·005 ± 0·002	2·9

TABLE 1. Densities and viscosities of the ambient fluid for jets of silicone oil 1

exit. The elvacite solution was a 9·8 % (by weight) solution of elvacite in diethyl malonate (DEM) and the elvacite itself is a polymethyl methacrylate polymer with a viscosity-average molecular weight of about 4×10^5. First we shall list the values of the relevant physical parameters for the liquids used in the experiments:

for silicone oil 1

$\mu = 10$ P, $\rho = 0·943$ g/cm^3, $\sigma = 21·2$ dyn/cm (into air);

for silicone oil 2

$\mu = 125$ P, $\rho = 0·972$ g/cm^3, $\sigma = 21·5$ dyn/cm (into air).

The silicone oil was injected into air and into various mixtures of water and alcohol. The viscosity of these mixtures was of the same order as the viscosity of water; that

Ambient fluid	Density difference silicone 2 (g/cm³)	Viscosity of ambient fluid (cP)
Air	0·972	—
100% alcohol	0·187	1·2
66% alcohol/water	0·102	2.3
42% alcohol/water	0·05	2·8
35% alcohol/water	0·023	2·8
27% alcohol/water	0·014	2·5

TABLE 2. Densities and viscosities of ambient fluids for silicone oil 2. The density of the alcohol mixtures was determined by weighing of known volumes.

Ambient fluid	Density difference elvacite/DEM (g/cm³)	Viscosity of ambient fluid (cP)
Air	1·067	—
Water	0·067	1
25% glycerol/water	0·005	2

TABLE 3. Densities and viscosities of ambient fluids for jets of elvacite

is, many orders of magnitude smaller than the silicone oil. The density difference and viscosity for the various mixtures used in the experiment are given in tables 1 and 2.

For the elvacite solution

μ (zero-shear viscosity) $= 9$ P, $\rho = 1·067$ g/cm³, $\sigma = 30·2$ dyn/cm (into air).
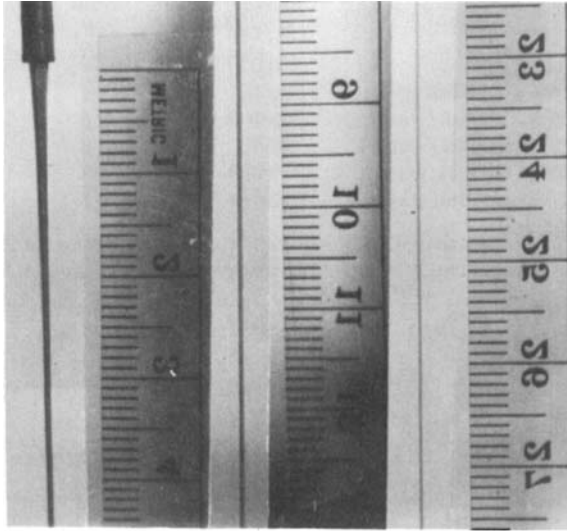The elvacite was injected into air and into various mixtures of water and glycerol. The viscosity of these mixtures is also of the order 10^{-2} P. The density difference for the various mixtures used in the experiment are given in table 3.

We were unsuccessful in finding values for the interfacial tension of the silicone oil into liquid. Ring-tensiometer measurements fail in liquid–liquid cases in which the surface tension is too small to measure.

Some typical raw data for the experiments are the photographs reproduced in figures 2 (*a–d*) (silicone 1) and 2 (*e–g*) (elvacite/DEM). The mass-flow rate for all the silicone 1 experiments was 0·16 g/s ($Q = 1·6/2\pi\rho = 0·027$ cm³/s) and for elvacite/DEM 0·61 g/s ($Q = 0·091$ cm³/s). A 1·78 mm inner diameter nozzle was used. The axial magnification of the true shape is different from the radial one owing to the curvature of the cylindrical container. The jet shapes are also plotted in figure 3 (silicone graph labelled [2], [3], [4], [5], [6]) and figure 4 (elvacite/DEM graph labelled [2], [3], [4]).

The interpretation of the experiments is best deferred until we have established some theory. Direct comparison with theory can be found at the ends of §§5 and 8. However, at this point it is perhaps useful to remind the reader that we are interested in the dynamics of the jet away from the pipe exit.

In the absence of gravity, $\epsilon = 0$ the jet attains a final uniform velocity $U = U_f$ and diameter $a = a_f$ (see e.g. Reddy & Tanner 1978; Trogdon & Joseph 1980, 1981). In
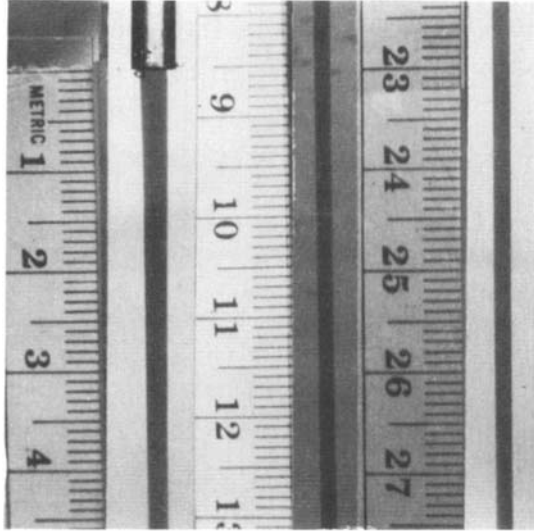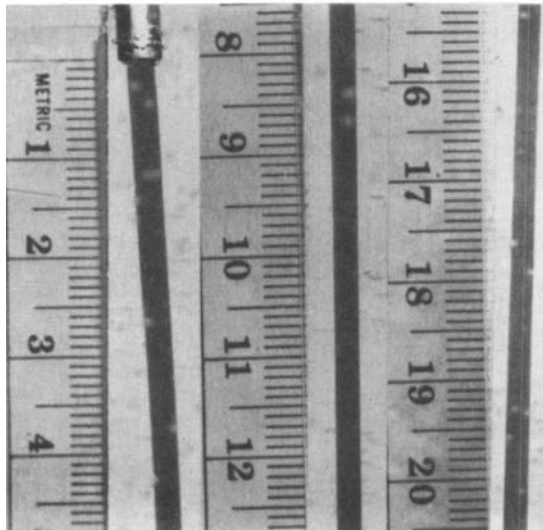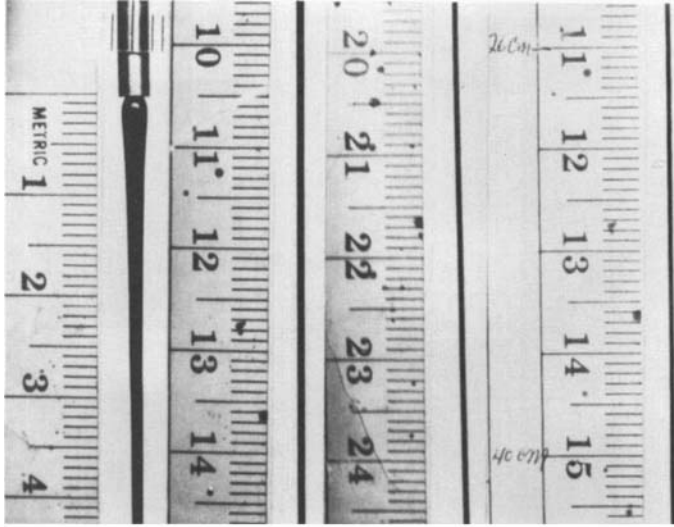
(a)
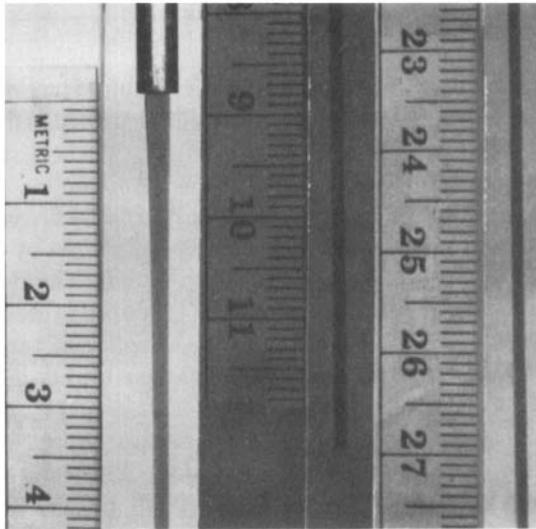
(b)

FIGURE 2(a, b). For caption see p. 451.
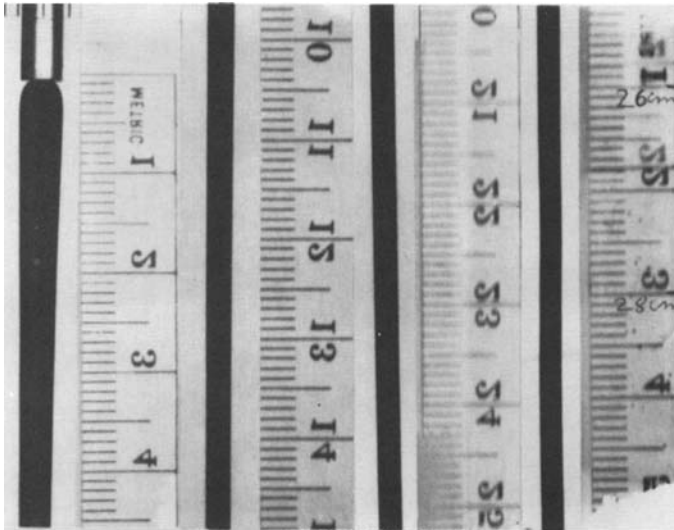
(c)

(d)

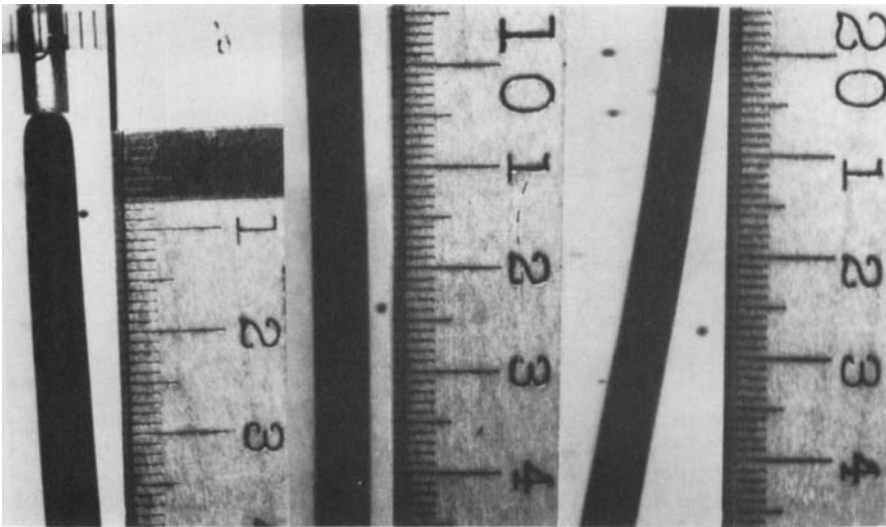FIGURE 2(c, d). For caption see p. 451.

(e)

(f)

FIGURE 2 (e, f). For caption see facing page.

(g)

FIGURE 2. Photographs of falling jets: (a)–(d) silicone 1; (e)–(g) elvacite/DEM.
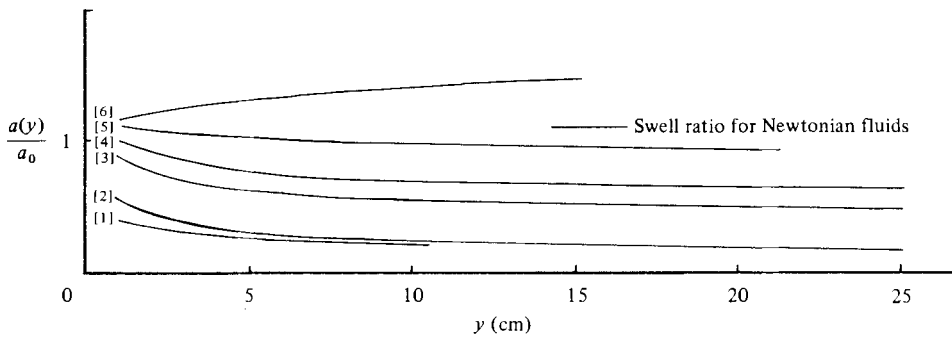

FIGURE 3. Jet shape for silicone oil 1 injected into air and various alcohol solutions: [1] equation (4.6); [2] $\epsilon\rho = \delta\rho = 0.943$; [3] 0.161; [4] 0.068; [5] 0.023; [6] 0.005. See table 1 for more information. The swell ratio $a(\infty)/a(0)$ for zero surface tension, gravity and Reynolds number is also indicated $(a(\infty)/a_0 = 1.113)$ (see Reddy & Tanner 1978; Trogdon & Joseph 1980, 1981).

this problem there is an important exit region, of just a few nozzle diameters, in which the rearrangement of the velocity profile and the jet diameter to their final constant values is nearly complete. This exit region is clearly evident in the photographs in figure 2. We want to exclude this small complicated region near the exit from the rest of the jet, which has a simpler dynamics.

For the elvacite experiments, the swell near the pipe exit is in good agreement with Tanner's (1970) prediction when injection is into air, but is about 30 % greater when injection is into fluids other than air. The same effect is observed with other visco-elastic fluids tested and appears to increase with the elastic shear compliance of the
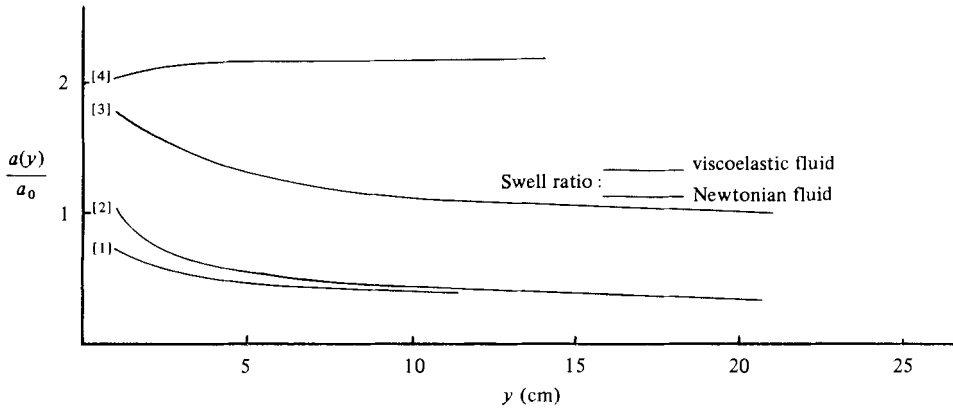
FIGURE 4. Jet shape for elvacite/DEM injected into air, water and glycerol solution: [1] equation (4.6); [2] $\epsilon\rho = \delta\rho = 1\cdot067$ (into air); [3] $0\cdot067$ (into water); [4] $0\cdot005$ (into glycerol solution). See table 3 for more information. We observe a very large die swell in the experiments labelled [3], [4]. The die-swell ratios for Newtonian fluid (Reddy & Tanner 1978; Trogdon & Joseph 1980, 1981) and for viscoelastic fluid (Tanner 1970) are also indicated above.

fluid. At one extreme, when $\epsilon = 0$, the flow a few diameters downstream is independent of r and x. At the other extreme, for jets of liquid into air with $\epsilon \approx 1$ the initial swelling does not appear to reach its die-swell value a_f because the effects of the acceleration of gravity in increasing U and decreasing a are manifest even quite close to the exit. On the other hand, jets of liquid into liquid are strongly influenced by the change of momentum of ambient liquid dragged along by the jet, and the velocities are slower and the jet radius larger than in the case of injection into air.

3. Momentum of the jet and entrained fluid

The equations governing the flow in the jet are

$$U = \mathbf{e}_x\, U(x,r) + \mathbf{e}_r\, W(x,r) \quad \text{(velocity)}, \tag{3.1a}$$

$$\mathbf{T} = -P\mathbf{I} + \mathbf{S} \quad \text{(stress)}, \tag{3.1b}$$

$$\partial_r(rW) + \partial_x(rU) = 0, \tag{3.2a}$$

$$\rho(W\,\partial_r\,U + U\,\partial_x\,U) = \partial_x\,T_{xx} + \frac{1}{r}\partial_r(rT_{rx}) + \rho g, \tag{3.2b}$$

$$\rho(W\,\partial_r\,W + U\,\partial_x\,W) = \partial_r\,T_{rr} + \partial_x\,T_{rx} + \frac{1}{r}(T_{rr} - T_{\theta\theta}). \tag{3.2c}$$

The same equations hold outside the jet. We use a tilde ($\tilde{U}$, $\tilde{\mathbf{T}}$, $\tilde{\rho}$ etc.) to designate variables in the fluid outside the jet. At the free surface $r = a(x)$ we require respectively that the normal component of velocity vanish and that jumps $[\![\,]\!] = (\,) - (\tilde{\,})$ in the velocity, the shear stress and the difference between jump in the normal stress and the surface-tension force ($\sigma =$ coefficient of surface tension) all vanish. When expressed in coordinate form these conditions may be written as

$$[\![U]\!] = 0, \tag{3.3a}$$

$$W - a'U = 0, \tag{3.3b}$$

$$a'[\![T_{rr}-a'T_{rx}]\!] + [\![T_{rx}-a'T_{xx}]\!] = 0, \tag{3.3c}$$

$$\frac{[\![T_{rr}+a'^2T_{xx}-2a'T_{xr}]\!]}{1+a'^2} + \frac{\sigma J'}{aa'} = 0, \tag{3.3d}$$

where $J = a/(1+a'^2)^{\frac{1}{2}}$, and $-p\mathbf{I}$ is the stress of the ambient fluid on the jet. Equation (3.3c) may be used to simplify (3.3d):

$$[\![T_{rr}-a'T_{xr}]\!] + \frac{\sigma J'}{aa'} = 0. \tag{3.4}$$

We now introduce the head

$$\Phi = p-\rho gx+\tilde{p}_0, \tag{3.5a}$$

$$\tilde{\Phi} = \tilde{p}-\tilde{\rho}gx+\tilde{p}_0, \tag{3.5b}$$

where $\tilde{p}_0$ is the pressure in the ambient fluid at the pipe exit at $x = x_0$, and the extra stress $\mathbf{S}$ into our equations. Then, in the jet we have

$$\rho(W\,\partial_r\,U + U\,\partial_x\,U) = \partial_x(-\Phi+S_{xx}) + \frac{1}{r}\partial_r(rS_{rx}), \tag{3.6a}$$

$$\rho(W\,\partial_r\,W + U\,\partial_x\,W) = \partial_r(-\Phi+S_{rr}) + \partial_x S_{rx} + \frac{1}{r}(S_{rr}-S_{\theta\theta}), \tag{3.6b}$$

whilst on $r = a(x)$

$$[\![\mathbf{U}]\!] = 0, \tag{3.7a}$$

$$W-a'U = 0, \tag{3.7b}$$

$$a'[\![S_{rr}-S_{xx}]\!] + (1-a'^2)[\![S_{rx}]\!] = 0, \tag{3.7c}$$

$$-\epsilon\rho gx + [\![-\Phi+S_{rr}-a'S_{rx}]\!] + \frac{\sigma J'}{aa'} = 0. \tag{3.7d}$$

To determine the hydrodynamics of the jet far downstream we shall need to relate the extra stress and velocity. Analysis shows that, though the velocity becomes large ultimately like x^α, $0 < \alpha \leqslant \frac{1}{2}$, strains decay at least like $x^{-\beta}$, $\beta > 0$. It therefore seems appropriate to use the small-strain-rate expressions $\mathbf{S} = \mu\mathbf{A}_1 + \alpha_1\mathbf{A}_2 + \alpha_2\mathbf{A}_1^2$ of the fluid of second grade. Here μ is the viscosity,

$$\mathbf{A}_1 = \nabla\mathbf{U}+\nabla\mathbf{U}^\mathrm{T}, \quad \mathbf{A}_2 = (\mathbf{U}.\nabla)\mathbf{A}_1 + \mathbf{A}_1.\nabla\mathbf{U} + (\mathbf{A}_1.\nabla\mathbf{U})^\mathrm{T},$$

and α_1 and α_2 are constants. In component form we have

$$S_{rr} = 2\mu\,\partial_r\,W + \alpha_1[2W\partial_{rr}\,W + 2U\partial_{rx}\,W + 4(\partial_r\,W)^2$$
$$+ 2(\partial_r\,U)^2 + 2\,\partial_r\,U\,\partial_x\,W] + \alpha_2[4(\partial_r\,W)^2 + (\partial_r\,U+\partial_x\,W)^2], \tag{3.9a}$$

$$S_{\theta\theta} = \frac{2\mu W}{r} + \alpha_1\left(2W\partial_r\frac{W}{r} + 2U\partial_x\frac{W}{r} + 4\frac{W^2}{r^2}\right) + 4\alpha_2\frac{W^2}{r^2}, \tag{3.9b}$$

$$S_{xx} = 2\mu\,\partial_x\,U + \alpha_1[2U\partial_{xx}\,U + 2W\partial_{rx}\,U + 4(\partial_x\,U)^2$$
$$+ 2(\partial_x\,W)^2 + 2\,\partial_x\,W\,\partial_r\,U] + \alpha_2[4(\partial_x\,U)^2 + (\partial_r\,U+\partial_x\,W)^2], \tag{3.9c}$$

$$S_{rx} = \mu(\partial_r\,U+\partial_x\,W) + \alpha_1[W(\partial_{rr}\,U+\partial_{rx}\,W) + U(\partial_{rx}\,U+\partial_{xx}\,W)$$
$$+ 3\,\partial_r\,W\,\partial_x\,W + 3\,\partial_r\,U\,\partial_x\,U + \partial_r\,U\,\partial_r\,W + \partial_x\,W\,\partial_x\,U]$$
$$+ \alpha_2[2\,\partial_r\,W\,\partial_x\,W + 2\partial_r\,U\,\partial_x\,U + 2\,\partial_r\,W\,\partial_r\,U + 2\partial_x\,W\,\partial_x\,U]. \tag{3.9d}$$

In §5 we will avoid making assumptions about the relation of stress to deformation in the hope of obtaining good jet-shape equations for unsteady problems and other problems in which the assumption of a second-order fluid is not justified.

454   *D. D. Joseph, K. Nguyen and J. E. Matta*

Equations (3.2), (3.6), (3.7) and (3.9) govern the motion at each point of the jet. We shall work with area-averaged equations expressing the conservation of linear and radial momentum of the jet derived (Joseph 1980) by integrating (3.6) across the cross-section of the jet, using (3.2) and (3.7). We get

$$\frac{d}{dx} \int_0^a [\rho U^2 + \Phi - S_{xx}] r \, dr = aa'[-\epsilon \rho g x + \Phi] + \sigma J' + a[\tilde{S}_{rx} - a'\tilde{S}_{xx}], \quad (3.10)$$

$$a'\frac{d}{dx} \int_0^a [\rho UW - S_{rx}] r \, dr = aa'[\epsilon \rho g x - \Phi] - \sigma J' + aa'[\tilde{S}_{rr} - a'\tilde{S}_{rx}] + a' \int_0^a [\Phi - S_{\theta\theta}] dr. \quad (3.11)$$

Area-averaged momentum equations also hold outside the jet. Here we get

$$\frac{d}{dx} \int_a^\infty [\tilde{\rho}\tilde{U}^2 + \Phi - \tilde{S}_{xx}] r \, dr = -a[\tilde{S}_{rx} + a'(\Phi - \tilde{S}_{xx})], \quad (3.12)$$

$$\frac{d}{dx} \int_a^\infty [\tilde{\rho}\tilde{W}\tilde{U} - \tilde{S}_{rx}] r \, dr = a[\Phi - \tilde{S}_{rr} + a'\tilde{S}_{rx}] + \int_a^\infty [\Phi - \tilde{S}_{\theta\theta}] dr. \quad (3.13)$$

We may eliminate boundary terms by adding (3.12) to (3.10) and (3.13) to (3.11). Thus

$$\frac{d}{dx} \left\{ \int_0^a [\rho U^2 + \Phi - S_{xx}] r \, dr + \int_a^\infty [\tilde{\rho}\tilde{U}^2 + \Phi - \tilde{S}_{xx}] r \, dr \right\} = -\epsilon \rho g x a a' + \sigma J', \quad (3.14)$$

$$\frac{d}{dx} \left\{ \int_0^a [r WU - S_{rx}] r \, dr + \int_a^\infty [\tilde{\rho}\tilde{W}\tilde{U} - \tilde{S}_{rx}] r \, dr \right\}$$
$$= \epsilon \rho g x a - \frac{\sigma J'}{a'} + \int_0^a [\Phi - S_{\theta\theta}] dr + \int_a^\infty [\Phi - \tilde{S}_{\theta\theta}] dr. \quad (3.15)$$

The terms involving $\epsilon \rho = g(\rho - \tilde{\rho}) > 0$ drive the flow. The jet falls because it is heavy. But (3.14) suggests that the dynamics of the jet can be strongly influenced by the change of momentum of entrained liquid outside the jet.

4. Torricelli formulas

We are going to obtain asymptotic formulas for the jet far downstream from the point x_0 of extrusion. For these large values of x, $x - x_0 \sim x$ no matter what may be the (fixed) value x_0. We get uniqueness of asymptotic formulas up to arbitrary translations of the origin of x. This type of lack of uniqueness comes from the fact that $\Phi(x, r)$ is determined by the global problem, and is only determined to within a constant by asymptotic analysis. In fact the equations are invariant under the transformation

$$\begin{bmatrix} \Phi(x, r) \\ x \end{bmatrix} \rightarrow \begin{bmatrix} \Phi(x - x_0, r) + \epsilon \rho g x_0 \\ x - x_0 \end{bmatrix}.$$

We are going to show that, if the ambient fluid is inviscid and dynamically passive, $\tilde{S} = \Phi = 0$, there is a unique asymptotic solution that perturbs the Torricelli limit.

The Torricelli limit arises for large values of x whenever the ambient fluid is inviscid and dynamically passive. To specify this limit it is convenient (but definitely not necessary) to consider the 'inviscid' flow of the viscous jet. In such a flow, the fluid is viscous but the viscous terms in the equations are inactive, as in potential flow of a viscous fluid. The flow in the falling jet is not inviscid at any finite x, but it tends

to an inviscid flow as $x \to \infty$. Suppose that the fluid is really inviscid. Then, the extra stress **S** vanishes, and, if we also assume that $\sigma = 0$, (3.10) reduces to

$$\left[\int_0^a (\rho U^2 + \Phi) \, r \, dr \right]' = -\epsilon \rho g x a a'. \qquad (4.1)$$

The Bernoulli equation for this flow (along streamlines) is

$$\tfrac{1}{2}\rho [U^2 + W^2] - \epsilon \rho g x + \Phi = C, \qquad (4.2)$$

where

$$Q = \int_0^{a(x)} U(x, r) \, r \, dr$$

is independent of x, and $|W| = o|U|$, $U(x, r) \to u(x)$ as $x \to \infty$ and $a(x) \to 0$. Hence in the limit

$$Q = \tfrac{1}{2} a^2 u. \qquad (4.3)$$

C is a pure constant which may be absorbed into Φ and hence put to zero in (4.2) without losing generality. So (4.1) may be written as

$$\left[\int_0^a (\tfrac{1}{2}\rho u^2 - \epsilon \rho g x) \, r \, dr \right]' = -\epsilon \rho g x a a', \qquad (4.4)$$

and, using (4.3),

$$\left(\frac{1}{a^2} \right)' = \frac{\epsilon \rho g}{2\rho Q^2} a^2,$$

$$a(x) = \left[\frac{2Q^2}{\epsilon g x} \right]^{\frac{1}{4}}. \qquad (4.5)$$

It follows now from (4.3) and (4.5) that

$$u(x) = (2\epsilon g x)^{\frac{1}{2}} \qquad (4.6)$$

is given by Torricelli's formula, modified for buoyancy. We get the same solutions in §5 when $x \to \infty$, even for non-Newtonian viscous fluids.

5. Perturbation of the Torricelli limit

The asymptotic expansion for large values of x of the functions $U(x, r)$, $W(x, r)$, $\Phi(x, r)$, $a(x)$ describing the flow in the falling jet follows from the observation that the continual acceleration of the jet due to gravity, coupled to the condition that the mass flux is constant, forces the radius of the jet to contract as x increases. In the limit, for large values of x, the variation of $U(x, r)$ across the cross-section of the jet must tend to zero so that the leading terms are independent of r. In fact, it is apparently possible to compute a unique asymptotic solution of (3.2), (3.7) with $\tilde{\mathbf{S}} = \tilde{\Phi} = 0$ and (3.9) in the form

$$\Psi(x, r) = \Sigma r^{2n} g_{2n}(x) = \sum_{n=1} r^{2n} \sum_{l=1} k_{2n}^{(l)} x^{-\frac{1}{4}l} - C x^{\frac{1}{2}} r^2,$$

$$a(x) = \sum_{n=1} a_n x^{-\frac{1}{4}n}, \quad C = (\tfrac{1}{2}\epsilon g)^{\frac{1}{2}}, \quad a_1 = \left(\frac{2Q^2}{\epsilon g} \right)^{\frac{1}{4}}, \qquad (5.1)$$

where

$$[U(x, r), (W(x, r)] = \frac{1}{r} [-\partial_r \Psi(x, r), \partial_x \Psi(x, r)].$$

Equations governing the $g_{2n}(x)$ are obtained by identifying independent powers of r in the equations that hold in the interior of the jet. At the boundary $r = a(x)$ we

use the expansions for $a(x)$ and $g_{2n}(x)$. Kaye & Vale (1969) also used the representation (5.1) in their study of Newtonian jets into air, but their actual calculation omits the effect of viscosity. We have carried out the identifications using (5.1) that are required to establish the asymptotic representations (5.19)–(5.23). We are not going to display the identification, which is tedious; instead we use the integrated equations of momentum (3.10) and (3.11) to determine the autonomous equation (5.18) for $a(x)$. We solve this equation in a series of fractional powers of x and then trace back through the derivation to obtain the other flow quantities.

To obtain the equation governing the asymptotic expansion of $a(x)$ for large x we first decompose the variables appearing in (3.10) and (3.11) as follows:

$$
\begin{bmatrix}
U(x,r) \\
-W(x,r)/r \\
\Phi(x,r) \\
S_{xx}(x,r) \\
S_{\theta\theta}(x,r) \\
S_{rr}(x,r) \\
S_{rx}(x,r) \\
J(x)
\end{bmatrix}
=
\begin{bmatrix}
u(x) \\
\tfrac{1}{2}u'(x) \\
\gamma(x) \\
\Gamma(x) \\
\theta(x) \\
\Omega(x) \\
\tau(x) \\
a(x)
\end{bmatrix}
+ r^2
\begin{bmatrix}
\tilde{u}(x) \\
\tfrac{1}{4}\tilde{u}'(x) \\
\tilde{\gamma}(x) \\
0 \\
0 \\
0 \\
0 \\
0
\end{bmatrix}
+
\begin{bmatrix}
\hat{u}(x,r) \\
\hat{w}(x,r) \\
\hat{\phi}(x,r) \\
\hat{\Gamma}(x,r) \\
\hat{\theta}(x,r) \\
\hat{\Omega}(x,r) \\
\hat{\tau}(x,r) \\
\hat{J}(x,r)
\end{bmatrix}
\begin{matrix}
(5.2a) \\
(5.2b) \\
(5.2c) \\
(5.2d) \\
(5.2e) \\
(5.2f) \\
(5.2g) \\
(5.2h)
\end{matrix}
$$

The functions in the first two columns are of leading order in powers of $x^{-\frac{1}{4}}$ and the functions in the last column are of higher order; $\hat{\Gamma}, \hat{\theta}, \hat{\Omega}, \hat{\tau}$ also have terms proportional to r^2 but the x-dependent functions of proportionality are of higher order. The assertions can be verified *a posteriori*. The volume flux

$$
Q = \int_0^{a(x)} U(x,r)\,r\,dr = \tfrac{1}{2}a^2[u(x) + \tfrac{1}{2}a^2\tilde{u}(x)] + \hat{f}_1(x) \tag{5.3}
$$

is a constant and

$$
\hat{f}_1(x) = \int_0^{a(x)} \hat{u}(x,r)\,r\,dr.
$$

Moreover

$$
Q^2 = \tfrac{1}{4}a^4[u^2(x) + a^2 u(x)\,\tilde{u}(x)] + \hat{f}_2(x) = \tfrac{1}{2}a^2\int_0^a U^2(x,r)\,r\,dr + \hat{f}_3(x), \tag{5.4}
$$

where (5.2) and (5.3) define $\hat{f}_2(x)$ and $\hat{f}_3(x)$ uniquely. We compute

$$
\int_0^a [\rho U^2 + \Phi - S_{xx}]\,r\,dr = \frac{2\rho Q^2}{a^2} + \tfrac{1}{2}a^2[\gamma(x) + \tfrac{1}{2}a^2\tilde{\gamma}(x) - \Gamma(x)] + \hat{f}_4(x), \tag{5.5}
$$

where $\hat{f}_4(x)$ is uniquely defined by (5.4), (5.2c) and (5.2d). Hence (3.10) becomes

$$
\frac{d}{dx}\left\{ \frac{2\rho Q^2}{a^2} + \tfrac{1}{2}a^2[\gamma(x) + \tfrac{1}{2}a^2\tilde{\gamma}(x) - \Gamma(x)] \right\} = -\epsilon\rho g x a a' + \sigma a' + \hat{f}_5(x), \tag{5.6}
$$

where $\hat{f}_5 = J'(x) - \hat{f}_4(x)$. In the same way, we compute from (5.2c, e)

$$
\int_0^{a(x)} [\Phi(x,r) - S_{\theta\theta}]\,dr = a[\gamma(x) + \tfrac{1}{3}a^2\tilde{\gamma}(x) - \theta(x)] + \hat{f}_6(x), \tag{5.7}
$$

and using (5.2a, b, f)

$$
\int_0^a [\rho UW - S_{rx}]\,r\,dr = -\tfrac{1}{6}\rho u(x)\,u'(x)\,a^3(x) + \hat{f}_7(x). \tag{5.8}
$$

Hence (3.11) becomes

$$-\tfrac{1}{6}\rho\frac{d}{dx}(u'ua^3) = \epsilon\rho gxa - \sigma + a[\gamma + \tfrac{1}{3}a^2\tilde{\gamma} - \theta] + \hat{f}_8(x), \tag{5.9}$$

where $\hat{f}_8(x) = -\hat{f}_7'(x) - \hat{J}'/a'$.

Turning next to (3.7c) with $\tilde{\Phi} = \mathsf{S} = 0$, we find that

$$\epsilon\rho gx + \gamma + a^2\tilde{\gamma} = \Omega(x) + \frac{\sigma}{a} + \hat{f}_9(x), \tag{5.10}$$

where $\hat{f}_9$ is defined uniquely by (3.7c) and (5.2). From (5.9) and (5.10) we can solve for $\tilde{\gamma}$ and find

$$\tilde{\gamma} = \frac{1}{4a^3}\rho\frac{d}{dx}(a^3uu') + \hat{f}_{10}(x), \tag{5.11}$$

where $\hat{f}_{10}$ are all the higher-order terms that arise after elimination. Now, using (5.11), we write (5.9) as

$$-\tfrac{1}{8}\rho\frac{d}{dx}(a^3uu') = \epsilon\rho gxa + a[\gamma + \tfrac{1}{2}a^2\tilde{\gamma} - \theta] - \sigma + \hat{f}_{11}. \tag{5.12}$$

Using (5.12), we eliminate $\gamma + \tfrac{1}{2}a^2\tilde{\gamma}$ in (5.6), and, after simplification, find that

$$\frac{d}{dx}\left\{\frac{2\rho Q^2}{a^2} + a^2(\theta - \Gamma) - \frac{a}{16}\frac{d}{dx}(a^3uu')\right\} = \tfrac{1}{2}\epsilon\rho ga^2 + \tfrac{1}{2}\sigma a' + \hat{f}_{12}. \tag{5.13}$$

Using (5.2) and (5.9), we find that

$$\theta - \Gamma = -3\mu u' - 3\alpha_1(uu')' - 3\alpha_2 u'^2 + \hat{f}_{13}. \tag{5.14}$$

Hence

$$2\rho Q^2\left(\frac{1}{a^2}\right)' - 3\{\tfrac{1}{2}[\mu u' + \alpha_1(uu')' + \alpha_2(u'^2)]a^2\}' - \tfrac{1}{16}[a(uu'a^3)]' = \tfrac{1}{2}\epsilon\rho ga^2 + \tfrac{1}{2}\sigma a' + \hat{f}_{14} \tag{5.15}$$

Finally we write

$$u(x) = \frac{2Q^2}{a^2} - \tfrac{1}{2}a^2\tilde{u} + \hat{f}_{15}, \tag{5.16}$$

where $\tilde{u}$ may be determined from the shear-stress condition (3.3b) written as

$$2a\tilde{u} - \tfrac{1}{2}au'' - 3a'u' + \hat{f}_{16} = 0. \tag{5.17}$$

Since the leading terms in U and a are of order $x^{\frac{1}{2}}$ and $x^{-\frac{1}{4}}$ respectively, $\tilde{u}$ is of order $x^{-\frac{5}{4}}$. We can therefore use $u(x) = 2Q/a^2$ in (5.15) without affecting the final result. It then follows from (5.15) that

$$-4\rho Q^2a' - \tfrac{1}{2}\epsilon\rho ga^5 + 6\mu Q[a''a^2 - a'^2a] - 48\alpha_2 Q^2\left[\frac{a'a''}{a} - 2\frac{a'^3}{a^2}\right]$$

$$+ 12\alpha_1 Q^2\left[a''' - 13\frac{a'a''}{a} + 20\frac{a'^3}{a^2}\right] + \tfrac{1}{2}\rho Q^2(a^2a''' - 5a'a'' + 4a'^3) = \tfrac{1}{2}\sigma a^3a' + \hat{f}_{17}(x). \tag{5.18}$$

We now set all of the $\hat{f}_i(x) = 0$, $i = 1, 2, ..., 17$. We solve the resulting equations as asymptotic power series in $x^{-\frac{1}{4}}$. Then we can verify that every $\hat{f}_i(x)$ is of lower order than the last term retained. All the unknowns may be generated from (5.18), and (5.1)

has a unique solution in powers of $x^{-\frac{1}{4}}$ with leading term given by (4.5). This solution is exhibited as (5.19)

$$a(x) = \frac{R_1}{x^{\frac{1}{4}}} + \frac{R_2}{x} + \frac{3(R_2^2 - R_3)}{2R_1 x^{\frac{7}{4}}} - \frac{R_4}{x^{\frac{9}{4}}}$$

$$+ \frac{2R_2^3 - \frac{159}{20}R_2 R_3}{R_1^2 x^{\frac{5}{2}}} + \frac{R_1^3}{32 x^{\frac{11}{4}}} - \frac{R_5 + 8R_2 R_4/R_1}{x^3} + O(x^{-\frac{13}{4}}), \quad (5.19a)$$

where
$$R_1 = \left(\frac{2Q^2}{\epsilon g}\right)^{\frac{1}{4}}, \quad R_2 = \frac{\sigma}{4\epsilon\rho g}, \quad R_3 = \frac{\mu Q}{\epsilon\rho g}, \quad R_4 = \frac{9\alpha_2}{16\rho}R_1, \quad R_5 = \frac{81\alpha_1}{112\rho}R_2.$$

The coefficients $R_1, \ldots, R_4$ are positive and R_5 is probably positive. The function $u(x)$ and the leading term in $\tilde{u}(x)$ can now be computed using (5.17) and (5.16). This gives

$$u(x) = \frac{2Q}{R_1^2}\left\{x^{\frac{1}{2}} - \frac{2R_2}{R_1 x^{\frac{1}{4}}} + \frac{3R_3}{R_1^2 x} - \frac{2R_4}{R_1 x^{\frac{3}{4}}} + \frac{\frac{77}{50}R_3 - 7R_2^3}{R_1 x^{\frac{7}{4}}} + \frac{1}{32}x^2 + \frac{4R_2}{R_1}\left[\frac{R_5}{R_2} + 7\frac{R_4}{R_1}\right]\frac{\rho}{x^{\frac{9}{4}}} + O(x^{-\frac{5}{2}})\right\},$$
$$(5.19b)$$

$$\tilde{u}(x) = \frac{Q}{2R_1^2}x^{-\frac{3}{2}} + O(x^{-\frac{9}{4}}). \quad (5.20)$$

Returning now to (5.10) and (5.11) we compute

$$\gamma = -\epsilon\rho g x + 4\epsilon\rho g \frac{R_2}{R_1}x^{\frac{1}{4}} + 4\epsilon\rho g\left(\frac{R_2^2}{R_1^2} - \frac{1}{4}\frac{R_3}{R_1^2}\right)x^{-\frac{1}{2}} + \frac{1}{4R_1^4}\left(\frac{224}{81}\rho\frac{R_5}{R_2} + \frac{16}{9}\rho\frac{R_4}{R_1}\right)x^{-1}$$

$$+ 4\epsilon\rho g\left[R_2\left(\frac{R_2^2}{R_1^3} - \frac{R_2}{R_1^2}\right) - \frac{1}{4}\frac{R_2 R_3}{R_1^2}\right]x^{-\frac{5}{4}} + \frac{3}{16}R_1^2 \epsilon\rho g x^{-\frac{3}{2}} + O(x^{-\frac{7}{4}}), \quad (5.21)$$

$$\tilde{\gamma} = r^2\left[-\frac{3}{16}\epsilon\rho g x^{-1} + O(x^{-\frac{7}{4}})\right]. \quad (5.22)$$

The error terms in (5.2) are

$$\begin{bmatrix} \hat{u} \\ \hat{w} \\ \hat{\phi} \\ \hat{\Gamma} \\ \hat{\theta} \\ \hat{\Omega} \\ \hat{\tau} \\ \hat{J} \end{bmatrix} = O\begin{bmatrix} x^{-2} \\ x^{-3} \\ x^{-\frac{7}{4}} \\ x^{-\frac{5}{2}} \\ x^{-\frac{5}{2}} \\ x^{-\frac{5}{2}} \\ x^{-\frac{3}{2}} \\ x^{-\frac{7}{2}} \end{bmatrix}.$$

Following Clarke (1968), we note that, when the distance $y = x - x_0$ from the point $y = 0$ of extrusion is introduced into (5.19), we get

$$a = \frac{R_1}{y^{\frac{1}{4}}} + \frac{R_2}{y} - \frac{x_0 R_1}{y^{\frac{5}{4}}} + O(y^{-\frac{7}{4}})$$

asymptotically, for large y. This shows that the asymptotic solution is uniquely determined only up to the first two terms which contain the principal effects of inertia and surface tension. Other effects, like viscosity and extensional stresses, depend on the undetermined constant x_0. In the case of jets of liquid into air there is good

agreement between experiments and the $y^{-\frac{1}{4}}$ law for values of y some pipe diameters downstream of the pipe exit at $y = 0$. This good agreement is evident in the graph labelled [1] in figures 3 and 4 and in some results published by Scriven & Pigford (1959) and Kay & Vale (1969).

The assumption $\tilde{\Phi} = \tilde{\mathbf{S}} = 0$ of this section is not good when $\epsilon \ll 1$. In this case the rate of change of the momentum of the ambient liquid entrained by the moving jet can be even larger than the change in the momentum of the jet itself. When $\tilde{\rho}$ is small ($\epsilon \approx 1$), however, as is the case with air, the momentum of the entrained fluid is small and does not strongly influence the observed dynamics. This is the reason why the analysis given in this section matches experiments on jets of liquid into air but not into other liquids.

Even if we confine our discussion to the case of jets of liquids into air, it is necessary to maintain a distinction between the jet-shape equation (5.18) and the seven-term asymptotic (for large x) solution (5.19) of (5.18). The jet-shape equation and the improved jet-shape equations derived in §6 evidently apply in intermediate regions where the flow is not yet asymptotic. This was shown by Kaye & Vale (1969), who studied a special case of (5.18) for air ($\rho \approx \delta\rho$) based on the assumption that r-variations of quantities on the left of (5.2) are zero and $\alpha_1 = \alpha_2 = 0$. Then they integrated the resulting equation, with $\sigma = 0$, subject to experimentally determined initial conditions for silicone oil into air. They got very good agreements for the jet shape in regions of not so large x where the asymptotic formulas fail.

6. Area-averaged equations

In §5 we used area-averaged equations to derive the asymptotic form of solutions that perturb the Torricelli limit. Now we shall examine more general approximations which follow from area-averaging of the equations of momentum and the assumption of weak r-dependence. We again confine our attention to the axisymmetric case, but the flow may be unsteady. For unsteady flow we must add $\rho\,\partial U/\partial t$ and $\rho\,\partial W/\partial t$ to the left-hand side of (3.2b, c) respectively. Moreover, the condition (3.3b), which says that the jet surface is a streamline, is replaced with the kinematic condition

$$W = \frac{\partial a}{\partial t} + a'U, \qquad (6.1)$$

where the prime denotes differentiation with respect to x. In the unsteady case we derive the following equations expressing the area-averaged balance of mass, axial momentum and radial momentum respectively:

$$\frac{1}{2}\frac{\partial}{\partial t}a^2 + \left[\int_0^a rU\,dr\right]' = 0, \qquad (6.2)$$

$$\rho\frac{\partial}{\partial t}\int_0^a rU\,dr + \left[\int_0^a (\rho U^2 + \Phi - S_{xx})\,r\,dr\right]' = -\rho\epsilon gxaa' + \sigma J' + a[\tilde{S}_{xr} + a'(\tilde{\Phi} - \tilde{S}_{xx})]_{r=a},$$
$$(6.3)$$

$$\rho\frac{\partial}{\partial t}\int_0^a rW\,dr + \left[\int_0^a (\rho WU - S_{rx})\,r\,dr\right]'$$
$$= \rho\epsilon gxa + \int_0^a (\Phi - S_{\theta\theta})\,dr - \frac{\sigma}{a'}J' + a[-\tilde{\Phi} + \tilde{S}_{rr} - a'\tilde{S}_{rx}]. \qquad (6.4)$$

Now we make our basic approximation, which may be described, loosely, as applicable to 'thin' jets or filaments. More precisely, we shall work in to-be-determined

regions of the jet where variations of the axial velocity $U(x, r, t)$ and 'pressure' $\Phi(x, r, t)$ are approximated by the first two terms of the expansion in powers of r^2 (see (5.2)). It will be enough to say that

$$U(x, r, t) \sim U(x, t) + r^2 \widetilde{U}(x, t), \qquad (6.5a)$$

$$\Phi(x, r, t) \sim \Phi(x, t) + r^2 \widetilde{\Phi}(x, t), \qquad (6.5b)$$

and that $\mathbf{S}(\mathbf{U})$ is determined by $\mathbf{U}$ alone. In this case we may reduce (6.2)–(6.4) and (3.7b, c) into five nonlinear equations in the five unknown functions $U(x, t)$, $\widetilde{U}(x, t)$, $\Phi(x, t)$, $\widetilde{\Phi}(x, t)$, $a(x, t)$.

The first step in the reduction is the determination of W corresponding to (6.5a) using (3.2a):

$$W(x, r, t) = -\tfrac{1}{2} r U'(x, t) - \tfrac{1}{4} r^3 \widetilde{U}'(x, t). \qquad (6.6)$$

Since $\mathbf{U}$ is now determined in terms of $U(x, t)$ and $\widetilde{U}(x, t)$, $\mathbf{S}[\mathbf{U}]$ is also determined in terms of these two functions. For example the stresses in a fluid of second grade may be determined from (3.9). S_{xx}, $S_{\theta\theta}$, S_{rr} and S_{rx}/r are polynomials in r^2 with coefficients depending on x and t. We may write in analogy to (5.2) that

$$\begin{bmatrix} S_{xx} \\ S_{\theta\theta} \\ S_{rr} \\ S_{rx}/r \end{bmatrix} = \sum_0^N r^{2m} \begin{bmatrix} \Gamma_m(x, t) \\ \theta_m(x, t) \\ \Omega_m(x, t) \\ \tau_m(x, t) \end{bmatrix}. \qquad (6.7)$$

Combining the expressions (6.5)–(6.7) with (6.2)–(6.4), we get

$$\frac{\partial}{\partial t} a^2 + \left[a^2 U + \frac{a^4}{2} \widetilde{U} \right]' = 0, \qquad (6.8)$$

$$\rho \frac{\partial}{\partial t} [\tfrac{1}{2} a^2 U + \tfrac{1}{4} a^4 \widetilde{U}] + \left[\tfrac{1}{2} \rho a^2 U^2 + \tfrac{1}{2} \rho a^4 U \widetilde{U} + \tfrac{1}{6} a^6 \rho \widetilde{U}^2 + \tfrac{1}{2} a^2 \Phi + \tfrac{1}{4} a^4 \widetilde{\Phi} - \sum_0^N \frac{a^{2m+2}}{2m+2} \Gamma_m \right]'$$
$$= -\rho \epsilon g x a a' + \sigma J' + a[\widetilde{S}_{xr} + a'(\Phi - \widetilde{S}_{xx})]_{r-a}, \qquad (6.9)$$

$$-\rho \frac{\partial}{\partial t} [\tfrac{1}{3} a^3 U' + \tfrac{1}{20} a^5 \widetilde{U}']$$

$$\quad - \left[\rho(\tfrac{1}{6} a^3 U U') + \tfrac{1}{20} \rho a^5 (\widetilde{U}' U + 2 U' \widetilde{U}) + \tfrac{1}{28} \rho a^7 \widetilde{U} \widetilde{U}' - \sum_0^N \frac{a^{2m+3}}{2m+3} \tau_m \right]'$$

$$\quad = \rho \epsilon g x a + \Phi a + \tfrac{1}{3} \widetilde{\Phi} a^3 - \sum_0^N \frac{a^{2m+1}}{2m+1} \theta_m - \frac{\sigma}{a'} J' + a[-\widetilde{\Phi} + \widetilde{S}_{rr} - a' \widetilde{S}_{xr}]_{r-a}. \qquad (6.10)$$

The interface conditions (3.7c, d) reduce respectively to

$$a' \sum_0^N a^{2m} (\Omega_m - \Gamma_m) + (1 - a'^2) \sum_0^N a^{2m+1} \tau_m = a'(\widetilde{S}_{rr} - \widetilde{S}_{xx}) + (1 - a'^2) \widetilde{S}_{xr}, \qquad (6.11)$$

$$\rho \epsilon g x - \Phi - u^2 \widetilde{\Phi} + \sum_0^N a^{2m} (\Omega_m - a a' \tau_m) + \frac{\sigma J'}{a a'} = -\widetilde{\Phi} + \widetilde{S}_{rr} - a' \widetilde{S}_{rx}, \qquad (6.12)$$

In the case of a Newtonian fluid $N = 1$ and

$$S_{rr} = 2\mu \frac{\partial W}{\partial r} = -2\mu [\tfrac{1}{2} U' + \tfrac{3}{4} r^2 \widetilde{U}'],$$

$$S_{xx} = 2\mu \frac{\partial U}{\partial x} = 2\mu[U' + r^2 \widetilde{U}'],$$

$$S_{\theta\theta} = 2\mu \frac{W}{r} = -2\mu[\tfrac{1}{2}U' + \tfrac{1}{4}r^2 \widetilde{U}'],$$

$$S_{xr} = \mu\left[\frac{\partial W}{\partial x} + \frac{\partial U}{\partial r}\right] = \mu[r(-\tfrac{1}{2}U'' + 2\widetilde{U}) - \tfrac{1}{4}r^3 \widetilde{U}''].$$

It is evident that $\widetilde{\boldsymbol{\Phi}}$ may be eliminated from this system, leaving four equations for four unknown functions $U(x,t)$, $\widetilde{U}(x,t)$, $\boldsymbol{\Phi}(x,t)$ and $a(x,t)$. We want to know the conditions under which these four nonlinear equations can give a good description of the dynamics of the jet.

Special cases of the equations for jets of liquid in air ($\delta\rho = \rho$, $\widetilde{\boldsymbol{\Phi}} = \widetilde{\mathbf{S}} = 0$) which arise when $\widetilde{\boldsymbol{\Phi}}(x,t)$ and $\widetilde{U}(x,t)$ are put to zero have been considered by various authors (Matovich & Pearson 1969; Pearson & Matovich 1969). In this r-independent case we get

$$\frac{\partial}{\partial t}a^2 + [a^2 U]' = 0, \tag{6.13}$$

$$\rho\frac{\partial}{\partial t}\tfrac{1}{2}a^2 U - [\tfrac{1}{2}a^2(\rho U^2 + \Phi - \Gamma_0)]' = -\rho egxaa' + \sigma J', \tag{6.14}$$

$$-\rho\frac{\partial}{\partial t}\tfrac{1}{3}a^3 U - \left[\tfrac{1}{3}a^3\left(\rho\frac{UU'}{2} - \tau_0\right)\right]' = \rho egxa + \Phi a - a\theta_0 - \sigma\frac{J'}{a'}, \tag{6.15}$$

$$a'(\Omega_0 - \Gamma_0) + (1 - a'^2)a\tau_0 = 0, \tag{6.16}$$

$$-(egx + \Phi) + \Omega_0 - aa'\tau_0 + \frac{\sigma J'}{aa'} = 0, \tag{6.17}$$

where $\Gamma_0, \Omega_0, \theta_0$ and τ_0 are determined by $U(x,t)$. Of course, it is not generally possible to solve these *five* equations for the three unknown functions U, Φ and a. The common practice is to ignore (6.16) and (6.17). (In fact, the first four terms of the asymptotic expansions (5.10) and (5.20) correspond to a solution which may be derived from (6.13)–(6.15) in the steady case and automatically satisfies (6.16) and (6.17) to the order considered).

In the steady case (6.13)–(6.15) reduce to

$$Q = \tfrac{1}{2}a^2 U(x) = \text{a constant independent of } x, \tag{6.18a}$$

$$[\tfrac{1}{2}a^2(\rho U^2 + \Phi - \Gamma_0)]' = -\rho egxaa' + \sigma J', \tag{6.18b}$$

$$-[\tfrac{1}{3}a^3(\tfrac{1}{2}\rho UU' - \tau_0)]' = \rho egxa + \Phi a - \theta_0 a - \frac{\sigma J'}{aa'}. \tag{6.18c}$$

Eliminating Φ, we find that

$$[\tfrac{1}{2}a^2(\rho U^2 + \theta_0 - \Gamma_0)]' - [a\{\tfrac{1}{6}a^3(\tfrac{1}{2}\rho UU' - \tau_0)\}']' = \tfrac{1}{2}\rho ega^2 + \tfrac{1}{2}\sigma J' - \tfrac{1}{2}\sigma a\left(\frac{J'}{a'}\right)'. \tag{6.19}$$

For second-order fluids, satisfying (3.9), we get

$$\theta_0 - \Gamma_0 = -3\{\mu U' + (\alpha_1 + \alpha_2)U'^2 + \alpha_1 UU''\}, \tag{6.20}$$

$$\tau_0 = \tfrac{1}{2}\{\mu U' + \alpha_1[U'U'' - UU'''] - \alpha_2 U'U''\}. \tag{6.21}$$
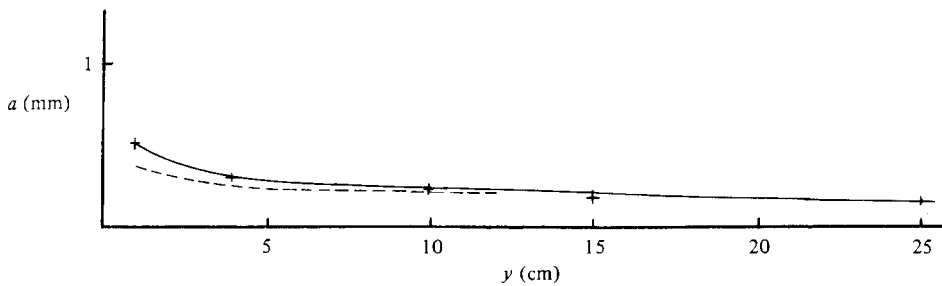
FIGURE 5. Jet shape for silicone oil 1 into air: ---, equation (4.6); ——, numerical integration of (6.22) with the right-hand side set to zero and taking two observed values $a(y = 1)$ and $a(y = 25)$ as prescribed; +, experimental data.

The average 'extensional' stress for the steady jet in regions far downstream is given by (6.20). Equations (6.18)–(6.21) may be combined into one single nonlinear jet-shape equation for $a(x)$. For Newtonian fluids we get

$$-4\rho Q^2 \frac{a'}{a^3} + 6\mu Q \left(\frac{a''}{a} - \frac{a'^2}{a^2} \right) - \tfrac{1}{2}\rho \epsilon g a^2 - \tfrac{1}{2}\sigma J = -\tfrac{1}{2}\sigma a \left(\frac{J'}{a'} \right)' - \left[a \left(\frac{5\rho Q^2 a'}{a^2} + \tfrac{1}{4}\mu Q a' \right)' \right]'$$

(6.22)

The nature of the simplification leading from the r-dependent equations (6.8)–(6.12) to (6.22) are such as to leave the region of validity of (6.22) obscure. Some authors (Kaye & Vale 1969) have treated (6.22) for the special case in which the right-hand side is negligible. The asymptotic analysis of §5 shows that the first four terms in the asymptotic expansion are asymptotic solutions of the equation arising from (6.22) when the right-hand side is set to zero.

There are also some numerical results which suggest that (6.22) is a valid equation under some circumstances. In particular, some good results have been obtained from (6.22) in two special cases of jets of liquid into air. Kaye & Vale (1969) integrated

$$-4\rho Q^2 \frac{a'}{a^3} + 6\mu Q \left(\frac{a''}{a} - \frac{a'^2}{a^2} \right) = \tfrac{1}{2}\rho g a^2$$

(6.23)

numerically for experimentally given initial conditions $a(x_0)$ and $a'(x_0)$ measured on jets of silicone oil into air. They got good agreement between the numerical calculations and the observed jet shape.

Kaye & Vale (1969) also did experiments with a Newtonian jet of low viscosity. But they could not get the jet shape from (6.23). (They should have included the surface-tension term $\tfrac{1}{2}J$.)

We have also integrated (6.23) for jets of silicone oil 1 into air ($\mu = 10$ P, $\epsilon \rho = \rho = 9.43$, $Q = 16$ g/s, $\sigma = 21.2$ dyn/cm). We use a two-point method for numerical integration, taking two observed values a_{y-1} and a_{y-25} as prescribed (see figure 5). We get good agreement between the experimental shape and the computed one even in regions in which the asymptotic solution fails. But we did not succeed in getting numerical computations based on (6.23) to agree with the jets of liquid into liquid because the momentum of the entrained liquid is important when the density of the ambient liquid is not small.

7. Boundary layers on the jet

To assess the effects of viscous drag on the momentum of the jet we now consider the dynamical effects of the ambient fluid in a boundary-layer approximation. We shall suppose that the viscosity of the jet is much larger than the viscosity of the ambient fluid, as is true in our experiments. In this case the shear of the ambient fluid may influence the momentum of the jet, but it does not induce strong variation of velocity across the cross-section of the jet. We shall further suppose that the ambient fluid is Newtonian and that the boundary layer is small in the sense that the pressure across it may be neglected.

$$\tilde{\Phi} = 0, \qquad (7.1)$$

and x-derivatives are smaller than r derivatives. Then

$$\tilde{U}\frac{\partial \tilde{U}}{\partial x} + \tilde{W}\frac{\partial \tilde{U}}{\partial r} = \tilde{\nu}\left(\frac{\partial^2 \tilde{U}}{\partial r^2} + \frac{1}{r}\frac{\partial \tilde{U}}{\partial r}\right), \qquad (7.2a)$$

$$\frac{\partial}{\partial x}r\tilde{U} + \frac{\partial}{\partial r}r\tilde{W} = 0, \qquad (7.2b)$$

where $\tilde{\nu} = \tilde{\mu}/\tilde{\rho}$ is the kinematic viscosity of the ambient fluid. We require that $\tilde{U}$ and $\tilde{W}$ be continuous at the jet surface $r = a(x)$ and that $a'(x)$ be small.

Using these approximations we may write

$$a(\tilde{S}_{xr} - a'\tilde{S}_{xx}) \approx \tilde{\mu}a\frac{\partial \tilde{U}}{\partial r}, \qquad (7.3)$$

and (3.10) becomes

$$\frac{d}{dx}\int_0^a (\rho U^2 + \Phi - S_{xx})\, r\, dr = -\epsilon\rho gaa' + \tilde{\mu}a\frac{\partial \tilde{U}}{\partial r}(x, a) + \sigma J'. \qquad (7.4)$$

It now follows directly from (7.2) and the conditions

$$\tilde{U}, \tilde{W} \to 0 \quad \text{as} \quad r \to \infty$$

that

$$a\tilde{\mu}\frac{\partial \tilde{U}(x, a)}{\partial r} = -\frac{d}{dx}\int_a^\infty \tilde{\rho}\tilde{U}^2\, r\, dr. \qquad (7.5)$$

Equation (7.5) says that the shear force at the jet surface is equal to the change in the momentum of the entrained liquid.

Now we seek to determine the velocity and diameter of the jet far downstream where r-variations of $\Phi = \phi$ and $U = u(x)$ in the jet are negligible. Then to leading order (3.11) may be written as

$$\epsilon\rho gxaa' - \sigma J' + aa'\gamma = 0, \qquad (7.6)$$

and (7.4) becomes

$$\frac{d}{dx}\left[\tfrac{1}{2}\rho a^2 u^2 + \frac{\sigma J' a}{a'} - \tfrac{1}{2}a^2 S_{xx}\right] = \tfrac{1}{2}\epsilon\rho ga^2 + \tilde{\mu}a\frac{\partial \tilde{U}}{\partial r} + \sigma J', \qquad (7.7)$$

$$Q = \tfrac{1}{2}ua^2.$$

When $\tilde{\mu} = 0$, we have the case studied in §4, and the leading asymptotic balance associated with (7.7) is

$$\frac{d}{dx}\rho a^2 u^2 = \epsilon\rho ga^2. \qquad (7.8)$$

The right-hand side of (7.8) can be interpreted as the weight of the jet per unit length, and the left-hand side gives the change of momentum per unit length.

We will show that, when $\tilde{\mu} \neq 0$, the leading balance is

$$\tfrac{1}{2}\epsilon\rho g a^2 + \tilde{\mu} a \frac{\partial \tilde{U}}{\partial r} = 0. \tag{7.9}$$

Equation (7.9) expresses the balance between the weight of the jet per unit length and the shear tractions on the jet wall.

We shall study the boundary-layer equations by a Kármán–Pohlhausen method. First we evaluate (7.2) on $r = a(x)$. We have

$$u(x) = \tilde{U}(x, a(x))$$

identically in x. Hence

$$u'(x) = \frac{\partial \tilde{U}}{\partial x} + a' \frac{\partial \tilde{U}}{\partial r},$$

$$\tilde{U} \frac{\partial \tilde{U}}{\partial x} + \tilde{W} \frac{\partial \tilde{U}}{\partial r} = u \left[u' - a' \frac{\partial \tilde{U}}{\partial r} \right] + W \frac{\partial \tilde{U}}{\partial r} = uu'$$

because $w - a'u = 0$ at $r = a$. Now we construct an approximate

$$\tilde{U}(x, r) = u(x)(1 - \eta)^2 f(\eta, x), \tag{7.10a}$$

$$f(\eta, x) = 1 + K_2(x)\eta^2, \tag{7.10b}$$

$$\eta = \frac{t - a}{\Delta(x)}, \quad \Delta(x) = \delta(x) - a(x) \tag{7.10c, d}$$

satisfying

$$\tilde{U}(x, \delta) = 0, \quad \tilde{U}'(x, \delta) = 0, \quad \tilde{U}(x, a) = u(x) \tag{7.11a, b, c}$$

$$\frac{\partial^2 \tilde{U}}{\partial r^2} + \frac{1}{a} \frac{\partial \tilde{U}}{\partial r} = \frac{uu'}{\tilde{\nu}} \tag{7.11d}$$

on $r = a(x)$. The conditions (7.11 a–c) are satisfied by (7.10), and (7.11) holds if

$$K_2(x) = \frac{u' \Delta^2}{2\tilde{\nu}} - 1 + \frac{\Delta}{a}.$$

Asymptotically we find that $K_2 = O(x^{\frac{1}{3}})$ and

$$K_2(x) \approx \Delta/a, \tag{7.12}$$

where the neglected terms, computed *a posteriori*, are $O(1)$ and $O(x^{-\frac{2}{3}})$.

Using (7.12) we find

$$\tilde{U}(x, r) \approx u(x)(1 - \eta)^2 \left[1 + \frac{\Delta}{a} \eta^2 \right], \tag{7.13}$$

$$\tilde{\mu} a \frac{\partial \tilde{U}}{\partial r}(x, a) = \tilde{\mu} au(x) \left(-\frac{2}{\Delta} \right) = -4 \frac{\tilde{\mu} Q}{\Delta a}. \tag{7.14}$$

The leading asymptotic balance (7.9) of momentum in the jet may now be written as

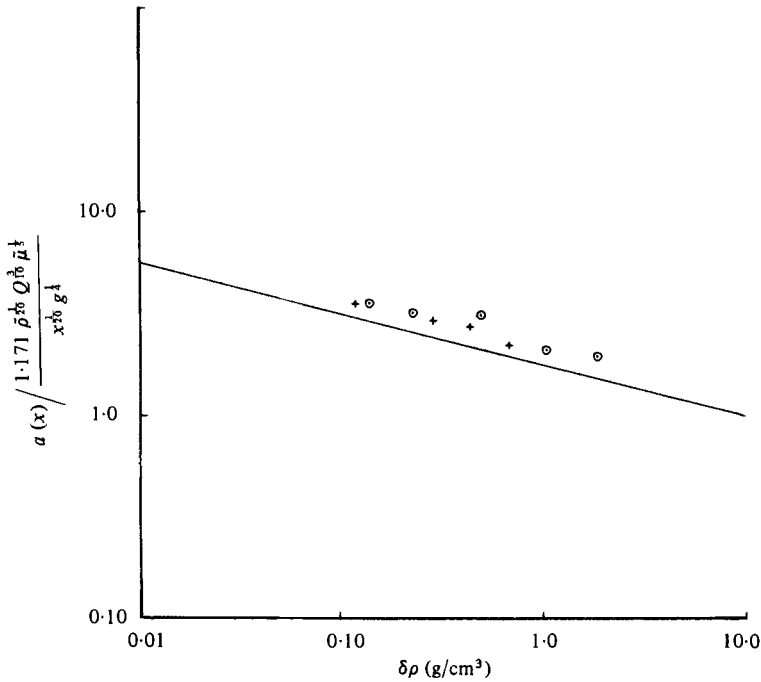$$\Delta \approx \frac{8\tilde{\mu} Q}{\epsilon\rho g a^3}. \tag{7.15}$$

FIGURE 6. Variation of jet radius with $\delta\rho$: ———, theoretical result,

$$R\bigg/\frac{1 \cdot 171\tilde{\rho}^{\frac{1}{20}}Q^{\frac{3}{10}}\tilde{\mu}^{\frac{1}{5}}}{X^{\frac{1}{10}}g^{\frac{1}{5}}} = (\delta\rho)^{-\frac{1}{4}};$$

+, experimental data for elvacite/DEM at $y = 25$ cm; $\odot$, experimental data for silicone oil 1 at $y = 25$ cm. In these plots the origin is taken at the orifice. The data show a slope of $-\frac{1}{4}$, in agreement with theory. The theoretical line can be made to pass through the experimental points by shifting the origin of x.

The balance of momentum of entrained fluid is given by (7.5) and may be evaluated using (7.13). We first compute

$$\int_a^\infty \tilde{\rho}\tilde{U}^2 r\,dr \approx \int_a^\delta \tilde{\rho}\tilde{U}^2 r\,dr = \tilde{\rho}u^2[\Delta^2(\tfrac{1}{30}+\tfrac{1}{140}K_2+\tfrac{1}{1260}K_2^2)+a\Delta(\tfrac{1}{5}+\tfrac{2}{105}K_2+\tfrac{1}{630}K_2)]. \quad (7.16)$$

To leading order $(\Delta^2 K_2^2 = O(x^{\frac{7}{10}})$ with neglected terms $O(x^{\frac{1}{2}})$, *a posteriori*) this is

$$\approx \frac{\tilde{\rho}u^2\Delta^4}{1260a^2} = \frac{\tilde{\rho}}{1260}4Q^2\frac{\Delta^4}{a^6} = \frac{\tilde{\rho}Q^6}{315}\left(\frac{8\tilde{\mu}}{\epsilon\rho g}\right)^4 a^{-18}. \quad (7.17)$$

Now, using (7.14) and (7.17), (7.5) may be written as

$$\frac{d}{dx}\left[\frac{\tilde{\rho}Q^6}{315a^{18}}\left(\frac{8\tilde{\mu}}{\epsilon\rho g}\right)^4\right] = \tfrac{1}{2}\epsilon\rho ga^2.$$

taking $a(\infty) = 0$, we get

$$a \approx 1 \cdot 171\left(\frac{\tilde{\rho}}{x}\right)^{\frac{1}{20}}\frac{Q^{\frac{3}{10}}\tilde{\mu}^{\frac{1}{5}}}{(\epsilon\rho g)^{\frac{1}{4}}}, \quad (7.18)$$
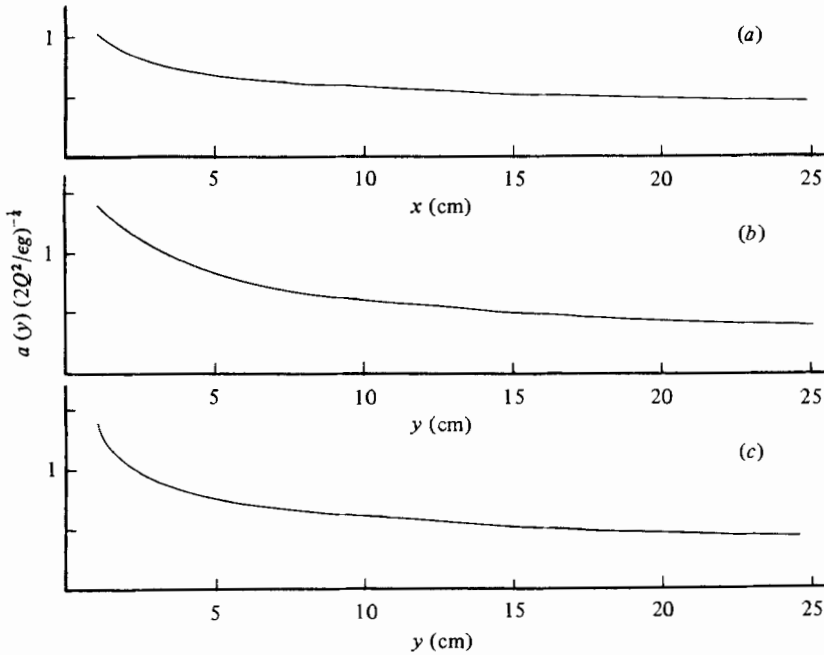
FIGURE 7. Comparison of the jet shape of liquid injected into air with Torricelli limit: (a) Torricelli limit, $a(y)(2Q^2/\epsilon g)^{-\frac{1}{4}} = y^{-\frac{1}{4}}$; (b) experimental data for silicone oil 1; (c) experimental data for elvacite/DEM. The three plots tend to coincide as $y \to \infty$.

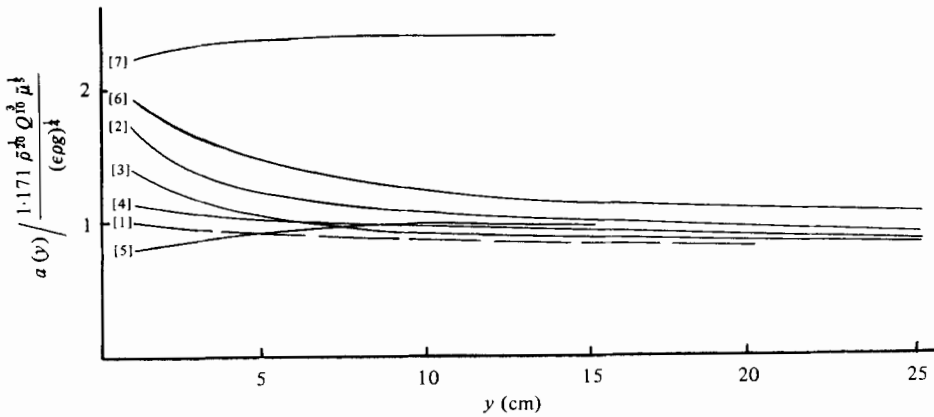FIGURE 8. Comparison of the jet shape of a liquid injected into another liquid: [1] theoretical,

$$a(y)\frac{1\cdot171\tilde{\rho}^{\frac{1}{20}}Q^{\frac{3}{10}}\tilde{\mu}^{\frac{1}{5}}}{(\epsilon\rho g)^{\frac{1}{4}}} = y^{-\frac{1}{20}}.$$

[2]–[5] experimental data for silicone oil 1 injected into alcohol solution; [2] $\epsilon\rho = \delta\rho = 0\cdot161$; [3] $0\cdot068$; [4] $0\cdot023$; [5] $0\cdot005$: [6], [7] experimental data for elvacite/DEM injected into water and glycerol solution; [6] $\epsilon\rho = \delta\rho = 0\cdot067$; [7] $0\cdot005$. In this figure the origin for the theoretical curve, which is arbitrary, is taken at the orifice. We count theory and experiments as being in agreement when it is possible to achieve agreement as $y \to \infty$ by changing the origin of y in [1]. The theory agrees with experiments [2]–[4] (silicone oil 1) and [6] (elvacite/DEM). When $\delta\rho$ is very small (experiments [5] and [7]) asymptotic regions are far from the orifice (eventually the accelerating jet must thin out). For [5] and [7], $\delta\rho = 0\cdot005$, the jet diameter has not yet entered a region of asymptotic dynamics suitable for comparison with [1].
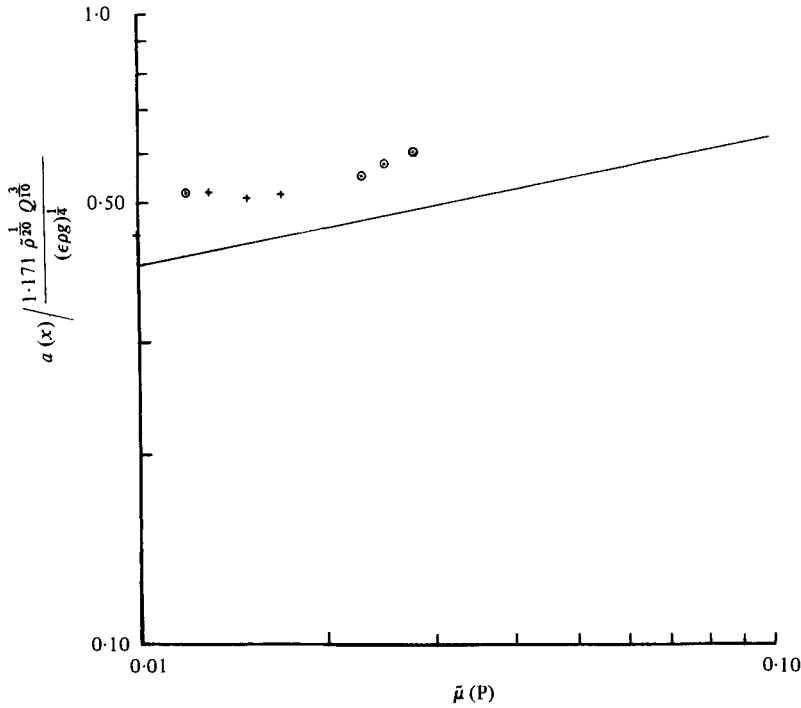
FIGURE 9. Variation of jet radius with $\tilde{\mu}$: ———, theoretical,

$$a \bigg/ \frac{1 \cdot 171 \bar{\rho}^{\frac{1}{20}} Q^{\frac{3}{10}}}{(\epsilon\rho g)^{\frac{1}{4}} x^{\frac{1}{4}}} = \tilde{\mu}^{\frac{1}{6}};$$

+, experimental data for elvacite/DEM; ⊙, experimental data for silicone oil 1. Jet radii are measured at $y = 25$ cm (the origin of x is taken at the orifice). The data show a slope of approximately $\frac{1}{6}$. The theoretical line can be made to pass through the experimental points by shifting the origin of x.

and when the viscosity $\tilde{\mu}$ of the ambient fluid is zero

$$a \approx \left[\frac{2Q^2}{\epsilon g x}\right]^{\frac{1}{4}}. \tag{7.19}$$

The $x^{-\frac{1}{20}}$ decay is much slower than the $x^{-\frac{1}{4}}$ decay, which must prevail at large x when $\tilde{\mu} = 0$. The asymptotic powers exhibited in (7.18) are, however, an approximation at best which is based on the notion that the dynamics of the entrained fluid may be treated by boundary-layer analysis, and that this analysis itself is adequately approximated by the Kármán–Pohlhausen procedure.

8. Comparison with experiments

The following points of comparison between theory and experiment merit emphasis.

(i) The experiment for jets of liquid into air are in good agreement with the Torricelli limit. The nature of these agreements has already been discussed at the end of §5.

(ii) The theory predicts that the jet radius scales with

$$\left(\frac{1}{\epsilon}\right)^{\frac{1}{4}}, \quad \epsilon = \frac{\rho - \tilde{\rho}}{\rho}.$$

This $\frac{1}{4}$-power singularity in the density difference holds uniformly in the viscosity $\tilde{\mu}$, even for $\tilde{\mu} = 0$. Therefore the $\frac{1}{4}$-power law is more robust than other features of the dynamics since it holds when the dynamics are dominated either by the changes of momentum of the jet (as in jets into a vacuum, or air) or by the entrained liquid outside the jet. The $\frac{1}{4}$-power law is in good agreement with our experiment summarized in figure 6.

(iii) For large values of x the jet radius is proportional to

$$\frac{1}{x^{\alpha}} \quad (\tfrac{1}{20} \leqslant \alpha \leqslant \tfrac{1}{4}).$$

The $\alpha = \frac{1}{4}$ results are verified for liquids into air, and $\alpha = \frac{1}{20}$ appears in the observations of liquids into liquids with $\epsilon \to 0$. The rate of change of momentum of the jet (given by the first term of (7.7), which by itself leads to $\alpha = \frac{1}{4}$) is still important at the largest values of x in the experiments. The shear-stress term, which is equal to the change of momentum of the entrained liquid, becomes more and more important as x is increased for fixed ϵ or as ϵ is decreased at a fixed x, with $\alpha(\epsilon)$ decreasing monotonically, apparently from $\frac{1}{4}$ to $\frac{1}{20}$. In reservation, we note that the value $\alpha = \frac{1}{20}$ is not yet evident for the smallest $\epsilon \approx 0.005$ because the diameter of the jet was still increasing at the largest x for which the jet was stable (see figures 7 and 8).

(iv) The jet radius appears to scale with the $\frac{1}{5}$ power of viscosity as predicted by (7.18) (see fig. 9).

Experimental results for the silicone oil 2 are in the same measure of agreement with theory as those already displayed for silicone oil 1 and will not be displayed here.

REFERENCES

CLARKE, N. S. 1969 The asymptotic effects of surface tension and viscosity on an axially-symmetric free jet of liquid under gravity. *Q. J. Mech. Appl. Math.* **22**, 247.

JOSEPH, D. D. 1980 An integral invariant for jets of liquid into air. *Arch. Rat. Mech. Anal.* **74**, 389.

KAYE, A. & VALE, D. G. 1969 The shape of a vertically falling stream of a Newtonian liquid. *Rheol. Acta* **8**, 1.

MATOVICH, M. A. & PEARSON, J. R. A. 1969 Spinning a molten threadline, steady-state isothermal viscous flows. *Ind. Engng Chem. Fund.* **8**, 512.

PEARSON, J. R. A. & MATOVICH, M. A. 1969 Spinning a molten threadline, stability. *Ind. Engng Chem. Fund.* **8**, 605.

REDDY, K. R. & TANNER, R. I. 1978 Finite element solution of viscous jet flows with surface tension. *Comp. Fluids* **6**, 83.

SCRIVEN, L. E. & PIGFORD, R. L. 1959 Fluid dynamics and diffusion calculations for laminar liquid jets. *A.I.Ch.E. J.* **5**, 397.

TANNER, R. I. 1970 A theory of die-swell. *J. Polymer Sci.* **8**, 2067.

TROGDON, S. A. & JOSEPH, D. D. 1980 The stick–slip problem for a round jet. I. Large surface tension. *Rheol. Acta* **19**, 404.

TROGDON, S. A. & JOSEPH, D. D. 1981 The stick–slip problem for a round jet. II. Small surface tension. *Rheol. Acta* **20**, 1.